EUROPEAN ORGANIZATION FOR NUCLEAR RESEARCH

CERN-ISR-VA/77-67
Closed distribution

THE DESIGN AND PERFORMANCE OF A 127° ELECTROSTATIC ENERGY ANALYZER AND THE MEASUREMENT OF THE ION ENERGY DISTRIBUTION IN AN ARGON GLOW DISCHARGE

by

A.G. Mathewson, K. Lee Li* and A. Grillot

[redacted]

*Student from Portsmouth Polytechnic, Portsmouth, Hants, GB.

Geneva, November 1977

1. INTRODUCTION

The final and most crucial part of the cleaning of the CERN Intersecting Storage Rings (ISR) vacuum chambers involves subjecting the interior surface to argon ion bombardment in a glow discharge[1]. In this process pure argon or argon/10% oxygen is admitted to the vacuum chamber at a pressure $\simeq 1 \times 10^{-2}$ torr and a glow discharge initiated by applying a positive DC voltage to a wire stretched axially along the chamber. The walls of the chamber are bombarded by ions whose energies depend on their radial position with respect to the anode wire when ionized. Obviously, a singly charged ion cannot have an energy greater than that corresponding to the applied voltage on the anode wire.

In this report the design, calibration and performance of an electrostatic energy analyzer is described and the actual ion energy distribution from a cleaning glow discharge measured at various pressures and applied anode voltages.

2. THE ELECTROSTATIC ANALYZER - THEORY

A schematic diagram of the analyzer is shown in Fig. 1. Basically it consists of two concentric cylindrical sectors with plates at each end containing entrance and exit slits. An inverse first power radial electrostatic field is set up between the sectors by applying a potential difference between them.

In polar coordinates (r,ϕ) with respect to the axis of the cylindrical sectors the potential at a point r,V(r), between the two sectors, neglecting end effects, is given by

$$V(r) = V_1 + \left[\frac{V_2 - V_1}{\ell n (b/a)}\right] \ell n \left(\frac{r}{a}\right) \qquad (1)$$

where a and b are the radii of curvature of the inner and outer cylinders respectively and V_1 and V_2 are the corresponding applied voltages. By symmetry and neglecting end effects for constant r the potential is independent of the polar angle .

The electric field $\mathcal{E}(r)$ is given by

$$\mathcal{E}(r) = \frac{V_2 - V_1}{\ell n (b/a)} \cdot \frac{1}{r} \qquad (2)$$

Under the influence of such an electric field a charged particle of mass m and charge q with initial velocity v at r_o (the entrance slit position) perpendicular to the electric field will describe a circular trajectory and pass through the

exit slit if

$$\frac{mv^2}{r_o} = \frac{V_2-V_1}{\ell n(b/a)} \cdot \frac{q}{r_o} \tag{3}$$

Writing $\Delta V = V_2-V_1$, the kinetic energy of the particle $\frac{1}{2}mv^2$ as E and with $M = \left[2\ \ell n(b/a)\right]^{-1}$ equation (3) reduces to the calibration equation

$$\frac{E}{q} = M\ \Delta V \tag{4}$$

The value of M may be found from the analyzer dimensions and for a known ΔV the energy which the analyzer will pass may be calculated from equation (4). Of course, for a given ΔV the analyzer will also pass particles of $\frac{2E}{2q}$, $\frac{3E}{3q}$, etc. Thus the analyzer measures the potential at which the transmitted ions were formed irrespective of their charge state.

Charged particles entering at $(r_o,0)$ with velocity v execute trajectories given by[2)]

$$\begin{aligned} r-r_o = r_o \Big[& \left(\frac{1}{\sqrt{2}} \sin \sqrt{2}\phi\right) + (1-\cos\sqrt{2}\phi)\beta \\ & + \left(-\frac{3}{8} + \frac{2}{3}\cos\sqrt{2}\phi - \frac{7}{24}\cos 2\sqrt{2}\phi\right)\alpha^2 \\ & + \left(\frac{1}{4} - \frac{5}{6}\cos\sqrt{2}\phi + \frac{7}{12}\cos 2\sqrt{2}\phi\right)\beta^2 \Big] \end{aligned} \tag{5}$$

to second order in α and β where α is the entrance angle shown in Fig. 1 and $\beta = \frac{v-v_o}{v_o}$ is the fractional velocity deviation from the tuned pass velocity $v_o = \sqrt{\frac{2EF}{m}}$. From equation (5) it can be seen that twin trajectories with small entrance angles $\pm\alpha$ and $\beta = 0$ cross after a deflection angle of $\phi = \pi/\sqrt{2} = 127^o\ 17'$.

For $\alpha = 0$ differentiation of equation (5) with respect to ϕ gives a maximum value for the resolution $\frac{r-r_o}{r_o}$ at again $\phi = \pi/\sqrt{2}$.

For these two reasons these types of energy analyzer usually have a deflection angle of $127^o\ 17'$.

It can also be shown[2)] from equation (5) that the maximum value of α is given by

$$\alpha_{max} = \frac{3\Delta S}{4r_o} \tag{6}$$

where ΔS is the exit slit width and r_o the radial position of the centre of the slit, and that the energy resolution $\frac{\Delta E}{E}$ is given by

$$\frac{\Delta E}{E} = \frac{\Delta S}{r_o} \tag{7}$$

for $\alpha = 0$.

It is convenient for practical reasons to place the entrance and exit slits at $r_o = \frac{a+b}{2}$. It is important that the equipotential surface through r_o be at zero volts since if it differs from zero, charged particles entering the analyzer will be either accelerated or decelerated and energy selection will follow from equ. (4), with E replaced by the actual kinetic energy within the analyzer. It is easily shown from equ. (1) that for this equipotential surface to be at zero at $r_o = \frac{a+b}{2}$ the ratio V_2/V_1 must satisfy

$$\frac{V_2}{V_1} = - \frac{\ell n\left(\frac{2b}{a+b}\right)}{\ell n\left(\frac{a+b}{2a}\right)} \tag{8}$$

3. THE ELECTROSTATIC ANALYZER - CONSTRUCTION DETAILS

The analyzer was made entirely from 316 L + N stainless steel. The inner and outer deflecting plates (a = 50 mm, b = 80 mm) consisted of stainless steel mesh spot welded to stainless steel frames machined from the solid to the correct radius of curvature. The height of the plates was 85 mm. Two further concentric solid guard plates served to collect under and over-deflected particles which could possibly reappear at the exit slit as a spurious signal.

The entrance and exit slits were identical (85 × 30 mm) with a slit width of 0.81 mm and a height of 10 mm. The centre of the slits was as far as possible at $r_o = \frac{a+b}{2} = 65$ mm and positioned symmetrically in the vertical position. Since the height of the analyzer was 85 mm and the slit height was 10 mm the field in this central region may be considered to be free from distortion due to the two solid plates at earth potential which closed the analyzer top and bottom. All four concentric electrodes, the entrance and exit slit plates and the top and bottom plates were all isolated electrically from each other and from ground. The current transmitted by the analyzer was measured by a Faraday cage coupled to an electrometer.

The analyzer and Faraday cage were housed in a stainless steel box which was connected to the discharge chamber via a 38 mm diameter tube as shown in Fig. 1. A 5 mm diameter hole in the chamber wall sampled the discharge ions which were collimated by a second 5 mm diameter hole positioned such that the value of the entry angle α was less than the 5.6^{o} maximum calculated from equ. (6).

Electrical connections to the interior were by UHV feedthroughs.

The voltages V_1 and V_2 were applied to the deflecting plates by means of the circuit shown in Fig. 1 where the values of R_1 and R_2 were chosen to give the correct V_2/V_1 ratio.

The discharge chamber was pumped by a turbomolecular pump and, since the operating pressure was $\simeq 1 \times 10^{-2}$ torr, to avoid discharge in the analyzer housing, where the deflecting plates could be at high voltage, a second pump was connected to the housing. The two 5 mm dia. holes provided sufficient impedance such that the pressure at the analyzer was low enough to avoid local discharge.

4. THE ELECTROSTATIC ANALYZER - CALIBRATION

The analyzer was calibrated using both electrons and ions from 10 to 510 eV. The sources are shown schematically in Fig. 2. The electron source was a small tungsten spiral heated by an AC current via an isolation transformer. The peak to peak voltage across the filament was 2.1 volts this therefore being the energy spread of the electrons. Floating the source to the appropriate negative voltage provided electrons of the required energy. A cup around the filament and at the same potential gave some directional control.

The ion source was of the potassium alumino silicate variety[3], was similar in dimensions to the electron source and was heated by the same circuit.

The energy spread of the ions was 1.8 eV and applying the appropriate positive high voltage to the source gave the required energy.

For calibration the sources were installed one at a time in the discharge chamber shown in Fig. 1 on a radius and pointing towards the hole in the chamber wall.

From the analyzer dimensions a = 50 mm, b = 80 mm and $r_o = \frac{a+b}{2} = 65$ mm (from equ. (8)) the ratio V_2/V_1 was found to be - 0.79 and the values of R_1 and R_2 were chosen to give $R_2/R_1 = 0.79$. The calibration constant $M = \left[2 \ln (b/a)\right]^{-1}$ has the value 1.064. In Fig. 3 are shown the theoretical and actual calibrations.

A least squares fit of the E versus ΔV data yielded M values of 1.087 and 1.076 for the ions and electrons respectively. The average value is 1.081 and it is this value we have used for the constant M. The actual and theoretical values differ by 1.57%.

From the definition, the fractional error in M, $\frac{\Delta M}{M}$, may easily be shown to be given by

$$\frac{\Delta M}{M} = \left[\frac{\Delta a}{a} - \frac{\Delta b}{b}\right] \frac{1}{\ell n(b/a)} \tag{9}$$

Assuming that the two radii of curvature of the deflecting plates are in error by 1 mm = Δa = Δb then from equ. (9) the percentage error in M is found to be 1.6% thus the difference between the calculated and measured values is explicable in terms of a 1 mm error in the radii of curvature. Such an error in a and b is not unreasonable since it was observed that after machining the supporting frames some distortion had occurred and a little difficulty was experienced in mounting these frames on the top and bottom plates in which holes corresponding to the correct radii of curvature had been drilled.

From equ. (7) the energy resolution $\frac{\Delta E}{E}$ was calculated to be 1.25×10^{-2}. Using the K^+ ion source whose energy spread was 1.86 eV the resolving power of the instrument was measured at 532 eV. The resulting energy distribution curve is shown in Fig. 4 where the ion current entering the Faraday cage is plotted against the pass energy of the analyzer. From the full width at half maximum (FWHM) the measured resolution was found to be 1.17×10^{-2}.

Since the bandwidth of the analyzer increases linearly with energy ($\Delta E = E \frac{\Delta S}{r_o}$) the actual transmitted current measured by the Faraday cage has this factor folded in. If n(E) is the actual ion energy distribution and I(E) is the measured transmitted ion current,

$$I(E) = \int_{E - \frac{\Delta E}{2}}^{E + \frac{\Delta E}{2}} n(E)\,dE \tag{10}$$

Thus to obtain the real distribution n(E) we must assume that n(E) is constant over the energy interval ΔE (the bandwidth). Equation (10) then becomes

$$I(E) = n(E)\,\Delta E \tag{11}$$

or

$$I(E) \propto n(E)\,E$$

and the measured ion current I(E) must be divided by E to give something proportional to n(E).

5. RESULTS

5.1 Pure Argon Discharge

In Fig. 5 is shown the measured argon ion energy distribution in a pure argon discharge at 3×10^{-3} torr for four different anode voltages, 380, 410, 430 and 480 V. The arrows indicate the energies corresponding to these voltages. It must be noted that the measured transmitted ion current is on a logarithmic scale and has already been divided by the energy E according to equation (11).

It is seen that the peak of the argon ion energy distribution is close to that corresponding to the anode wire voltage. The high energy tail is due to the fact that there was an 8 volt peak to peak ripple on the applied anode voltage, the measured voltage being, of course, some average of this. In addition the resolution at 500 eV is about 6 eV thus ions with energies up to about 10 eV above those corresponding to the nominal wire voltage may be transmitted by the analyzer. Apart from the main peak no other structure was evident.

In Fig. 6 is shown the argon ion energy distribution at a constant anode voltage of 380 V for three different pressures 3×10^{-3}, 6×10^{-3} and 7.9×10^{-3} torr. Again the peak of the distribution is situated at an energy corresponding to the anode wire voltage. Over the pressure range investigated, the position of the peak of the argon ion energy distribution remained unchanged. At 6×10^{-3} and 7.9×10^{-3} torr some structure superimposed on the background was observed around 150 eV and 330 eV but at the lower pressure the energy distribution was smooth. Relative to the main peak these other weak structures were about a factor of one thousand less in intensity. On all these curves the ordinate is in eV although it must be remembered that the actual ion energy may be a multiple of that indicated due to higher charge states of the ion.

5.2 Argon/10% Oxygen Discharge

Since all of the discharge cleaning of the ISR vacuum chambers is carried out using an argon/10% oxygen mixture, the ion energy distribution of ions from this gas mixture was then measured. The measured ion energy distribution is shown in Fig. 7 for a discharge at 1.4×10^{-2} torr for three different anode wire voltages 410, 440 and 480 V, the corresponding energies being shown by the arrows.

This time it is seen that there are two peaks in the energy distribution, one corresponding almost to the anode voltage as in the pure argon case and the other at about half that energy.

At a constant anode voltage of 480 V, changing the pressure from 3×10^{-3} torr to 1.4×10^{-2} torr resulted in the energy distributions shown in Fig. 8. Over this pressure range the positions of the peaks did not change but on increasing the pressure the low energy peak increased while the high energy peak decreased.

It is tempting to associate this additional low energy peak as being due to oxygen ions in the discharge; however, confirmation of this hypothesis requires that the ion species be identified at all energies in the distribution. A convenient way of doing this is to replace the Faraday cage by a quadrupole mass analyzer. However, this necessitated the construction of a completely new energy analyzer chamber so in the meantime a quadrupole mass analyzer was mounted in the place of the 127^{o} energy analyzer and all the ions coming from the discharge identified, irrespective of energy.

5.3 Ion Identification by Quadrupole Mass Analysis

A pure argon discharge was first investigated and the results are shown in Fig. 9 where at a constant pressure of 6.2×10^{-3} torr the anode voltage was varied between 350 and 426 V. Only two ion species were observed, at m/e = 40 and 20 corresponding to Ar^{+} and Ar^{++} respectively. The ratio of Ar^{+} to Ar^{++} increased from about 4.3 at 350 V to about 5.8 at 426 V.

Keeping the anode voltage constant at 380 V and changing the pressure from 3×10^{-3} to 1.3×10^{-2} torr produced a striking effect on the Ar^{+}/Ar^{++} ratio as shown in Fig. 10. At 3×10^{-3} torr the ratio of Ar^{+} to Ar^{++} was about 9.7 whereas at 1.3×10^{-2} torr it was 1.

At other mass numbers no further ion species were seen.

Running a discharge with argon/10% oxygen at a constant pressure of 8.8×10^{-3} torr and varying the anode voltage between 350 and 480 V produced the series of mass spectra shown in Fig. 11. Only four ion species were observed, at m/e = 16, 20, 32 and 40 corresponding to O^{+} and/or O_2^{++}, Ar^{++}, O_2^{+} and Ar^{+} respectively. At this gas pressure the most prominent peak was that due to O^{+} and/or O_2^{++} followed by O_2^{+}, Ar^{+} and Ar^{++}. Exceptionally at 480 V the Ar^{+} peak was higher than the O_2^{+} peak.

Keeping the anode voltage constant at 440 V and varying the pressure (Fig. 12) between 3×10^{-3} torr and 1.5×10^{-2} torr produced a dramatic change in the relative abundance of the four ion species. At 3×10^{-3} torr the Ar^{+} peak

predominated while at 6×10^{-3} torr the Ar^+ and O^+/O_2^{++} peaks were equal in height. Increasing the pressure further to 8.8×10^{-3} torr and 1.5×10^{-2} torr resulted in almost complete disappearance of the Ar^+ leaving O^+/O_2^{++} as the dominant ion species in the discharge. Thus by judicious choice of the pressure the bombarding ion species may be selected.

6. CONCLUSION

Energy analysis of the ions produced in a pure argon discharge revealed that the majority of the ions reach the wall with an energy corresponding to that of the voltage on the central anode wire. Changing the pressure or the wire voltage had little effect on the shape of the ion energy distribution.

Identification of the ions present revealed only A^+ and A^{++} the relative concentrations of which depended slightly on wire voltage, the ratio Ar^+ to Ar^{++} increasing with voltage at constant pressure. At constant wire voltage the Ar^+/Ar^{++} ratio depended strongly on pressure being about 9 at 3×10^{-3} torr and 1 at 1.3×10^{-2} torr. No other ion species were observed.

The energy distribution of the ions produced in an argon/10% oxygen discharge revealed two peaks, one close to the energy corresponding to the wire voltage and a second at about half that energy. Increasing the pressure from 3×10^{-3} torr to 1.4×10^{-2} torr at a constant wire voltage resulted in a decrease of the high energy peak and an increase of the low energy peak.

Four ion species O^+ and/or O_2^{++}, Ar^{++}, O_2^+ and Ar^+ were identified in the argon/10% oxygen discharge. At 8.8×10^{-3} torr the O^+/O_2^{++} peak dominated and at 350 V was followed by O_2^+, Ar^+ and Ar^{++}, the order changing to O^+/O_2^{++}, Ar^{++}, O_2^+, Ar^{++} at 480 V. At a constant voltage of 440 V changing the pressure from 3×10^{-3} torr, where the Ar^+ peak dominated, to 1.5×10^{-2} torr resulted in a very low Ar^+ peak and a very large O^+/O_2^{++} peak.

In conclusion it appears that the situation is rather involved, thus the measurements will be repeated with the quadrupole mass analyzer in the place of the Faraday cage and the energy distribution for each individual ion species measured as a function of pressure and anode wire voltage. In addition, it is appreciated that change, exchange and recombination effects may further complicate the interpretation.

These measurements will be the subject of a future publication.

7. ACKNOWLEDGEMENTS

The authors are indebted to Drs. Calder, Fischer and Hilleret, for support and useful discussion. One of us, K. Lee Li is grateful to CERN for the award of a studentship.

REFERENCES

1. R. Calder, A. Grillot, F. Le Normand and A. Mathewson, 7th Int. Vacuum Congress, Vienna, 12-16th Sept., 1977.

2. P. Bryce, R.L. Dalglish and J.C. Kelly, Can. J. of Physics, Vol. 51, 1973, 574.

3. Marie-Hélène Achard, CERN Report, CERN-ISR-VA/76-34, 1976.

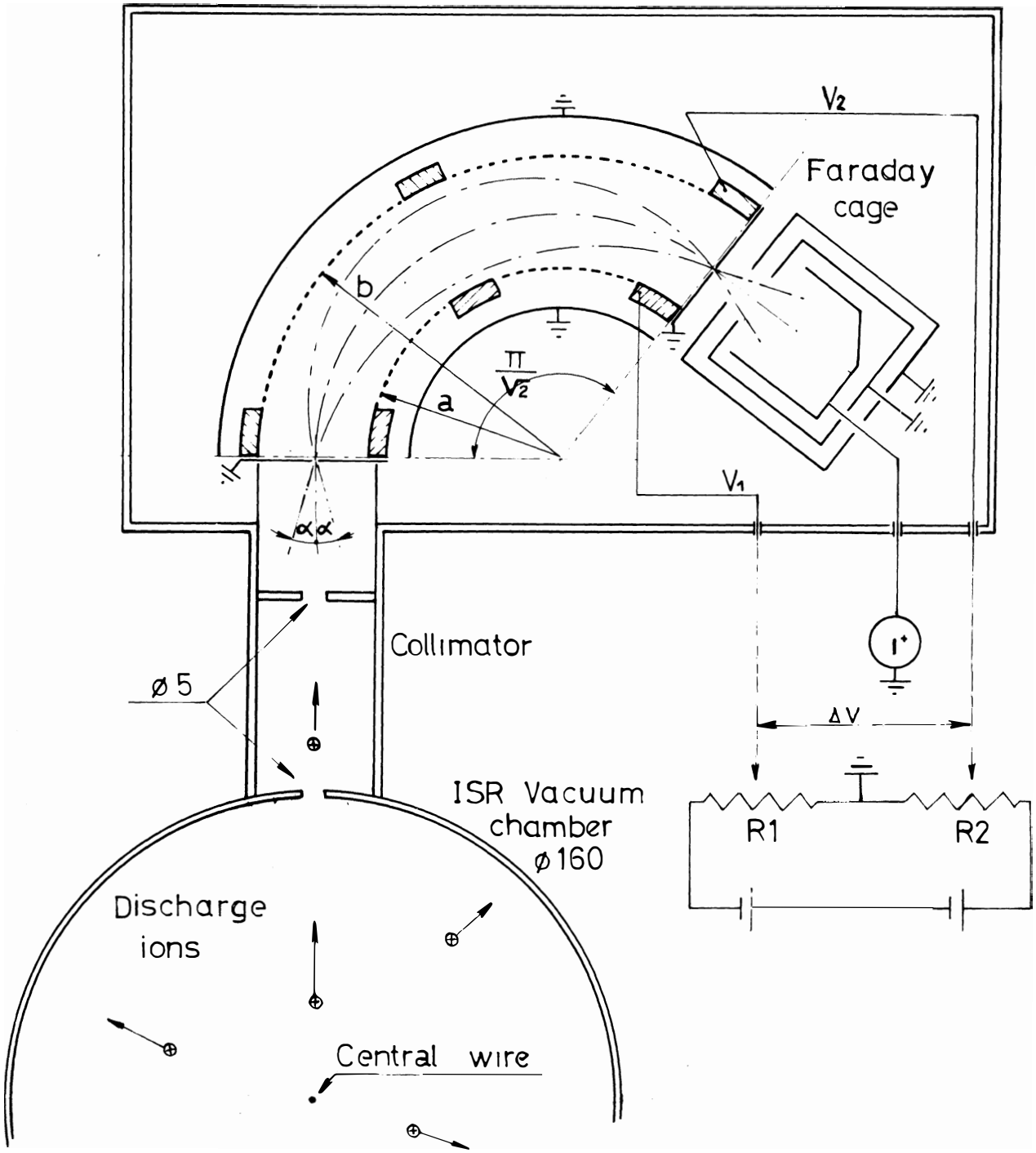
V2
Faraday
cage
b
π
V2
a
V1
α α
Collimator
ø 5
I+
ΔV
ISR Vacuum
chamber
ø 160
R1
R2
Discharge
ions
Central wire

FIGURE 1

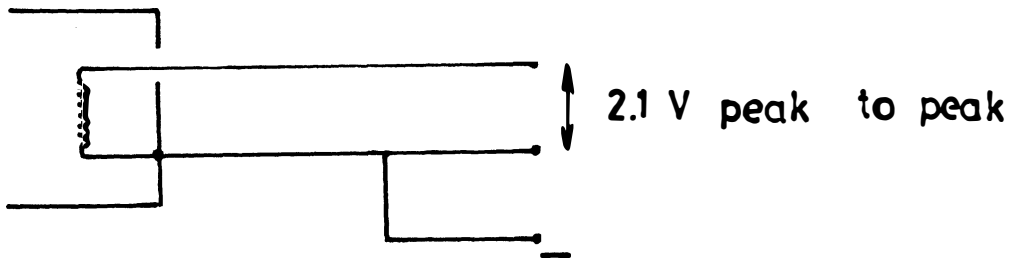

Electron source

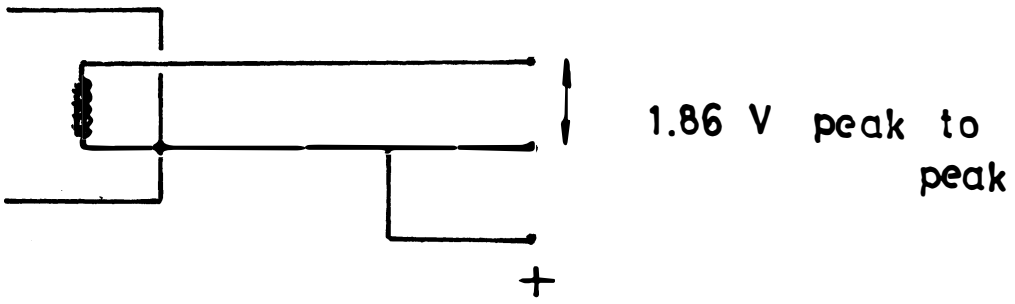

Ion source

FIGURE 2

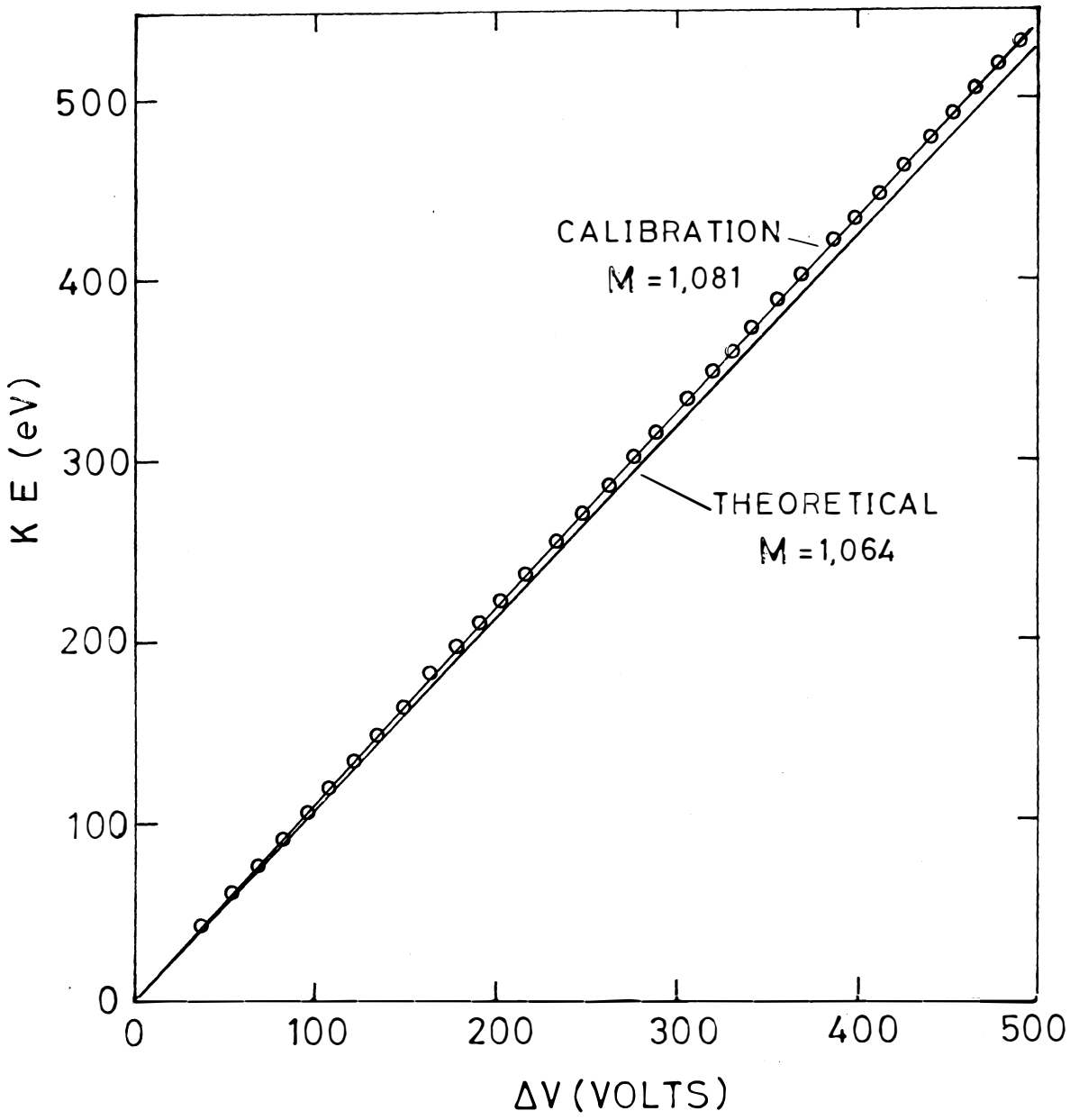
500
400
300
200
100
0
KE (eV)
0
100
200
300
400
500
ΔV (VOLTS)
CALIBRATION
M = 1,081
THEORETICAL
M = 1,064

FIGURE 3

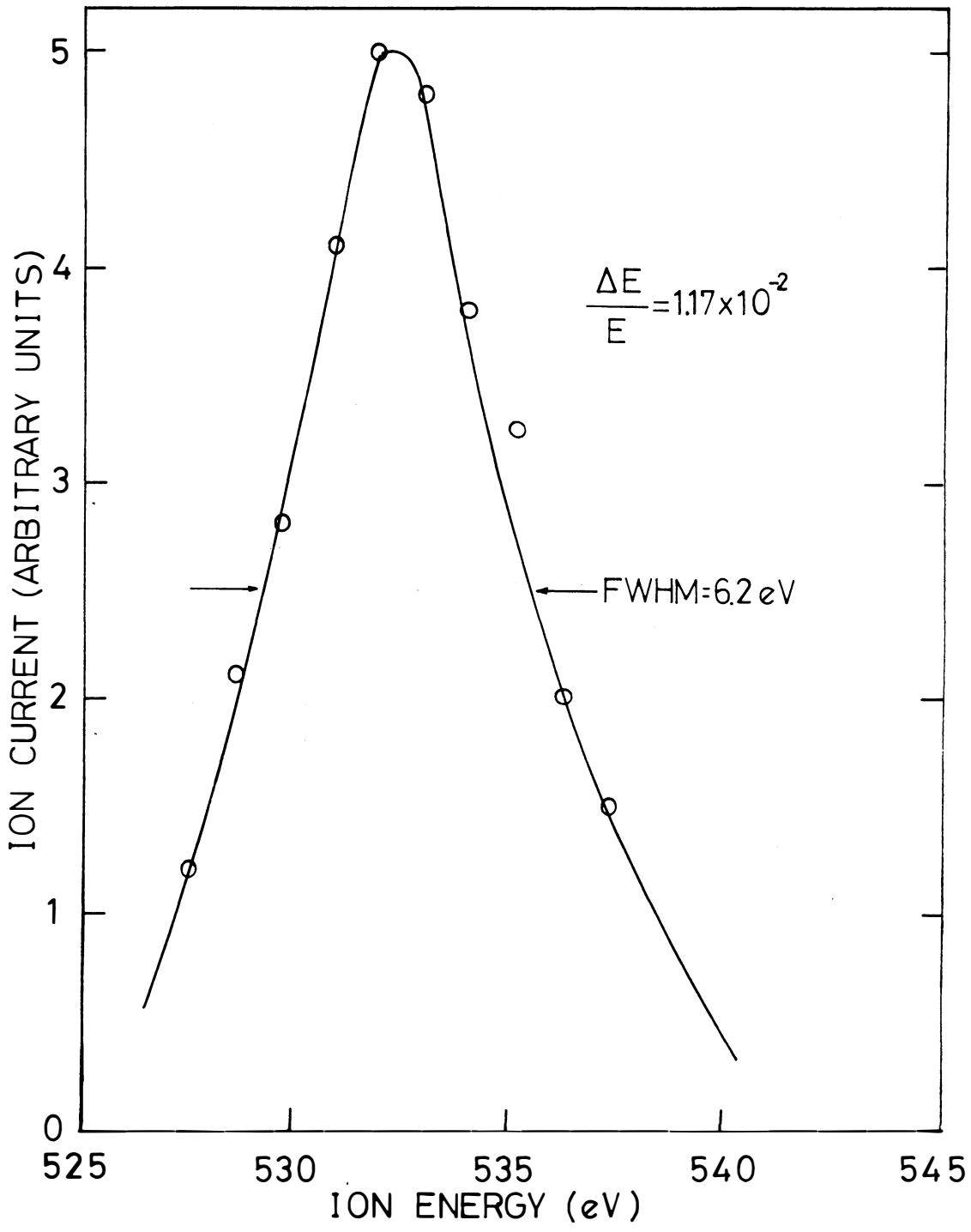
ION CURRENT (ARBITRARY UNITS)
0
1
2
3
4
5
525
530
535
540
545
ION ENERGY (eV)
ΔE/E = 1.17x10^-2
FWHM=6.2 eV

FIGURE 4

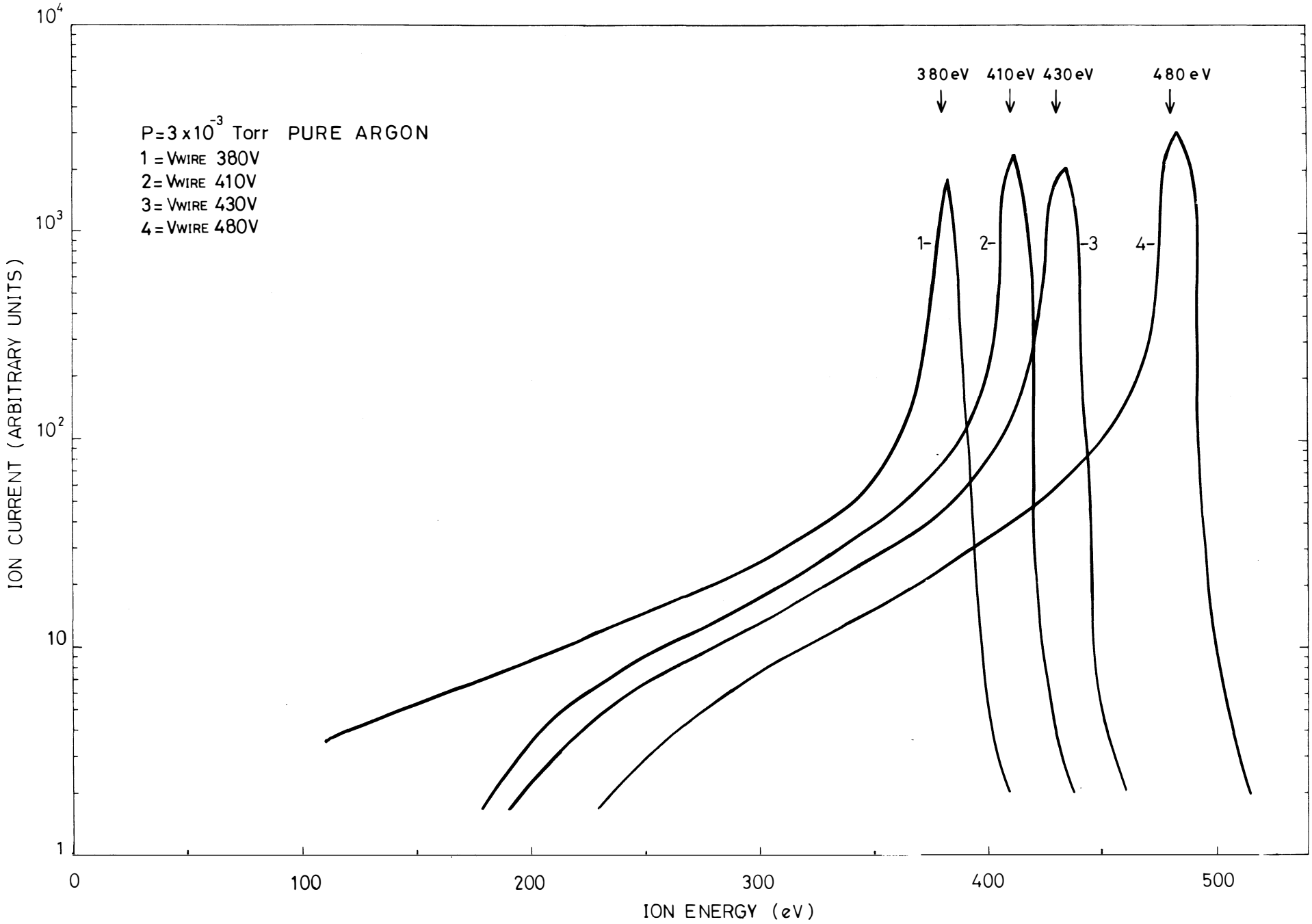
10^4
10^3
10^2
10
1
ION CURRENT (ARBITRARY UNITS)
P=3 x 10^{-3} Torr PURE ARGON
1 = VWIRE 380V
2 = VWIRE 410V
3 = VWIRE 430V
4 = VWIRE 480V
380eV
410eV
430eV
480eV
1-
2-
-3
4-
0
100
200
300
400
500
ION ENERGY (eV)

FIGURE 5

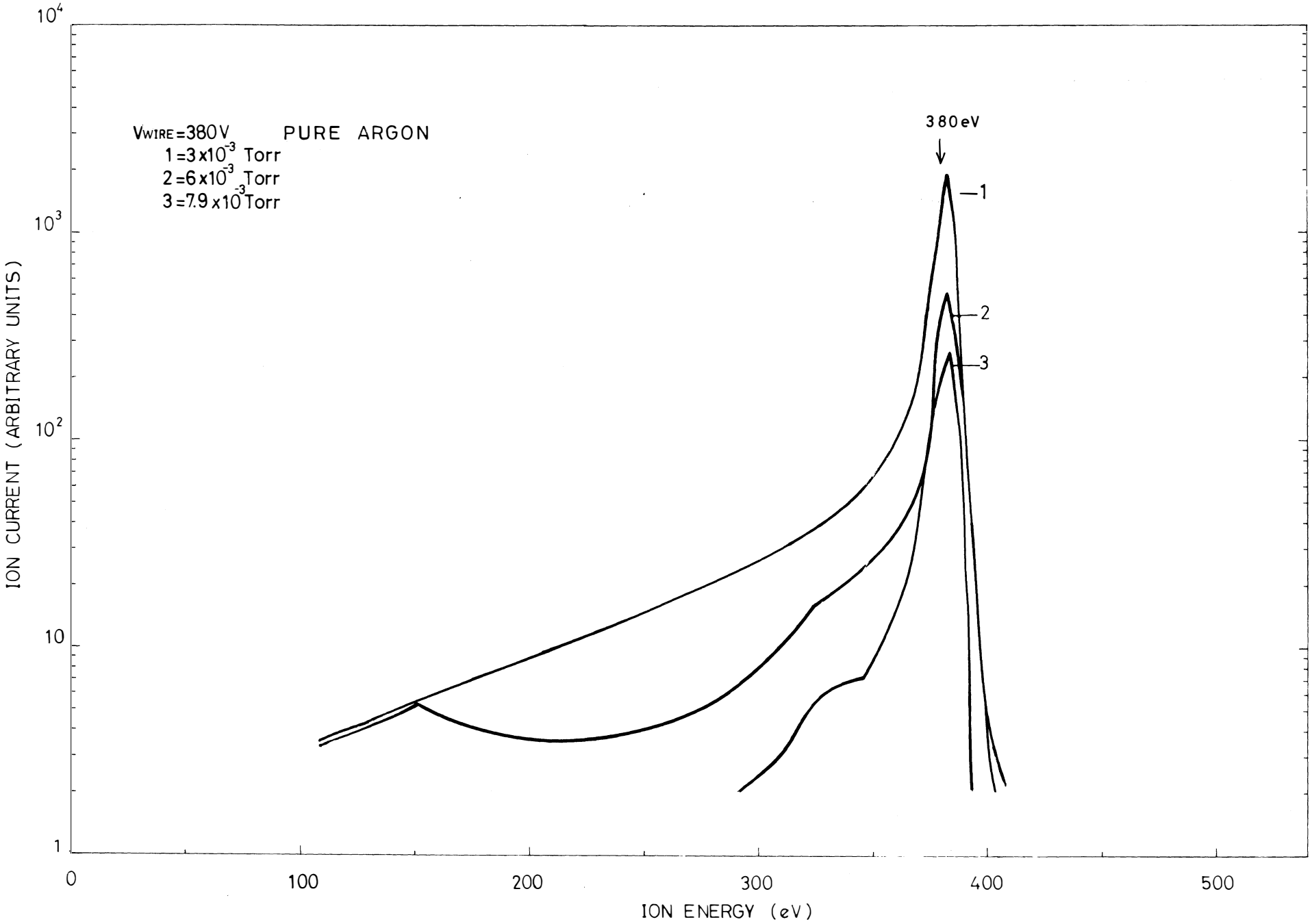
10^4
10^3
10^2
10
1
ION CURRENT (ARBITRARY UNITS)
V_{WIRE}=380V PURE ARGON
1=3x10^{-3} Torr
2=6x10^{-3} Torr
3=7.9x10^{-3}Torr
380eV
1
2
3
0
100
200
300
400
500
ION ENERGY (eV)

FIGURE 6

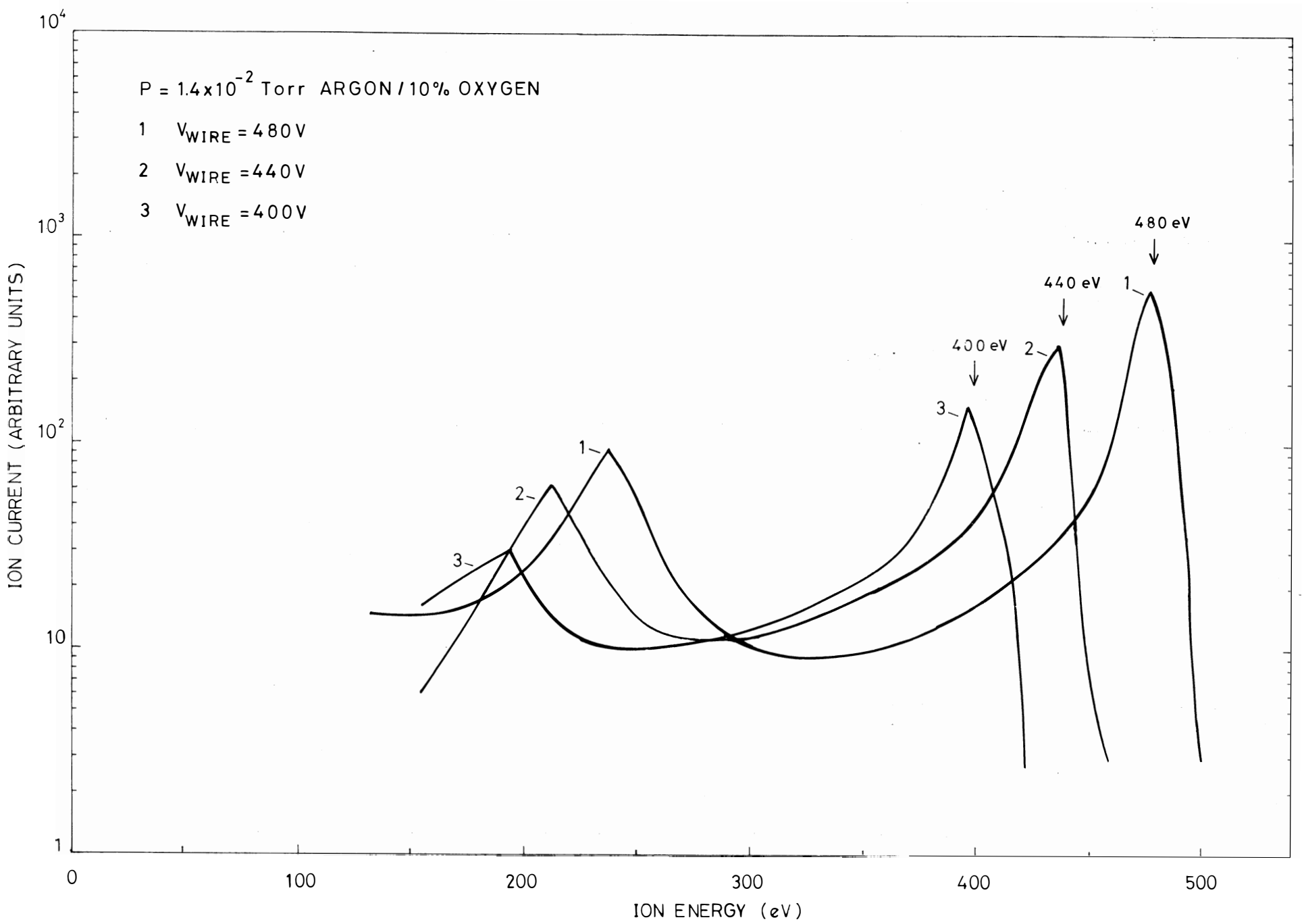
P = 1.4x10^-2 Torr ARGON / 10% OXYGEN
1 V_WIRE = 480 V
2 V_WIRE = 440 V
3 V_WIRE = 400 V
480 eV
440 eV
400 eV
ION CURRENT (ARBITRARY UNITS)
ION ENERGY (eV)
10^4
10^3
10^2
10
1
0
100
200
300
400
500

FIGURE 7

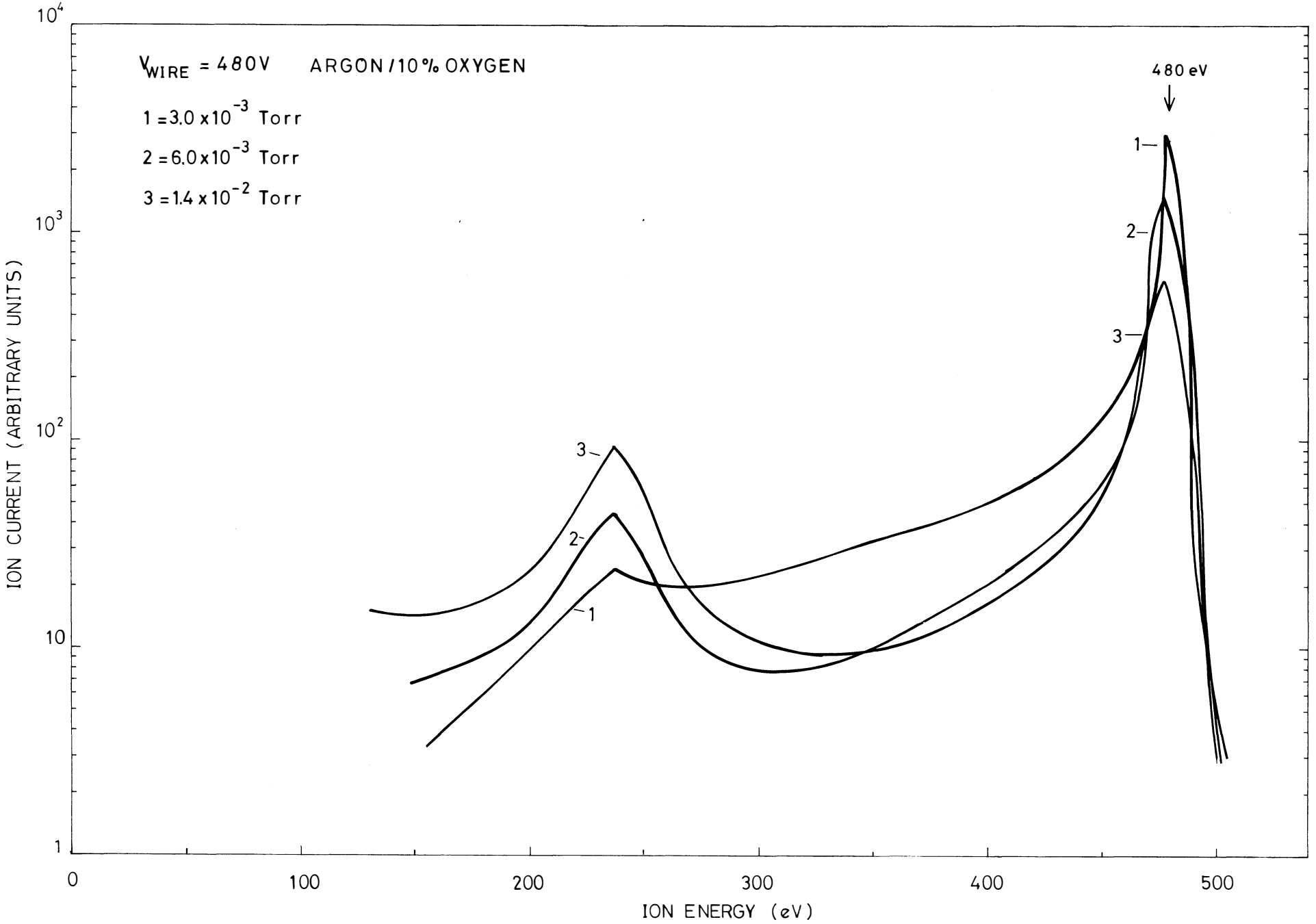
V_{WIRE} = 480V ARGON / 10% OXYGEN
1 = 3.0 x 10^{-3} Torr
2 = 6.0 x 10^{-3} Torr
3 = 1.4 x 10^{-2} Torr
480 eV
ION CURRENT (ARBITRARY UNITS)
ION ENERGY (eV)
10^4
10^3
10^2
10
1
0
100
200
300
400
500

FIGURE 8

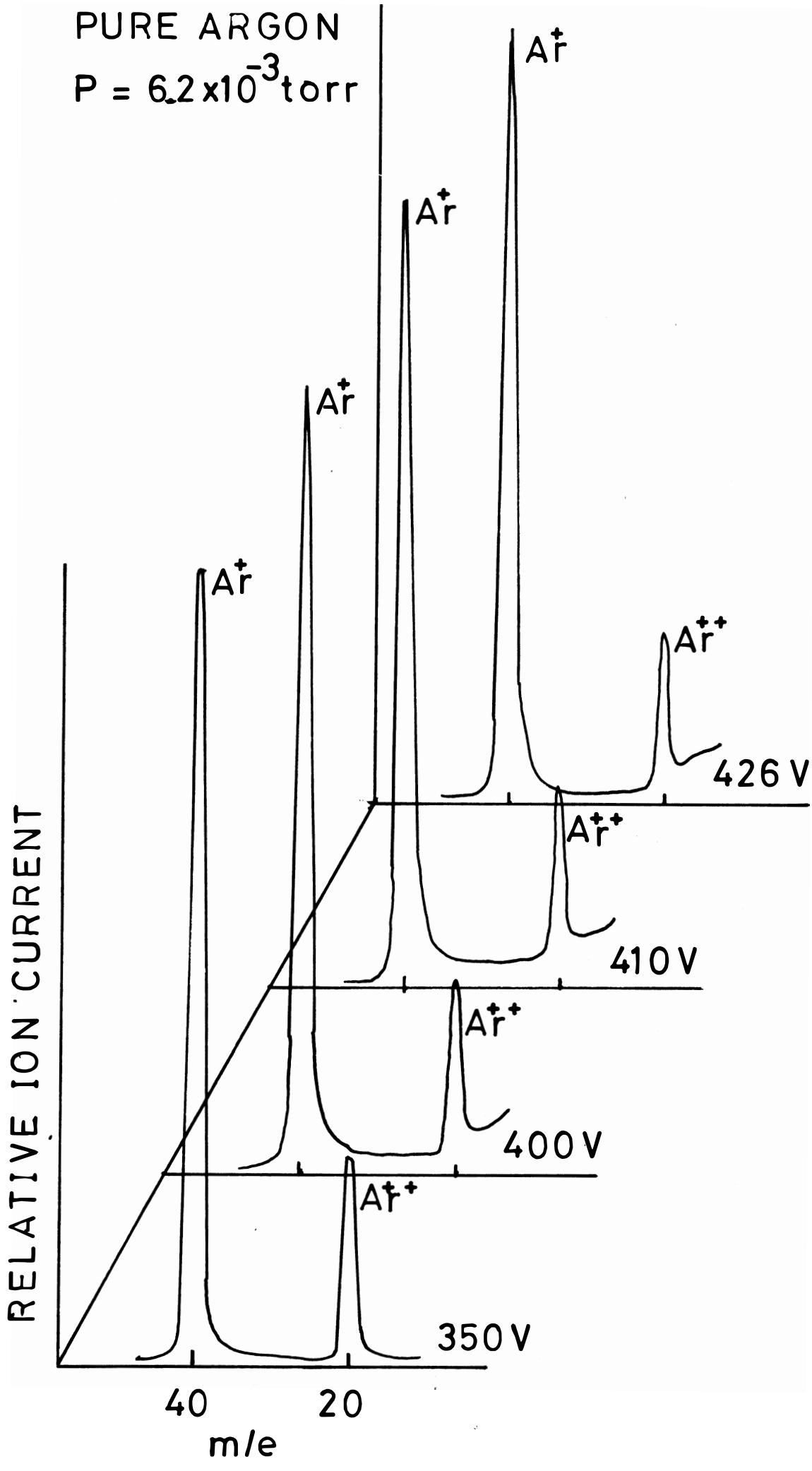
PURE ARGON
P = 6.2x10⁻³ torr
Ar+
Ar+
Ar+
Ar+
Ar++
426 V
Ar++
410 V
Ar++
400 V
Ar++
350 V
RELATIVE ION CURRENT
40
20
m/e

FIGURE 9

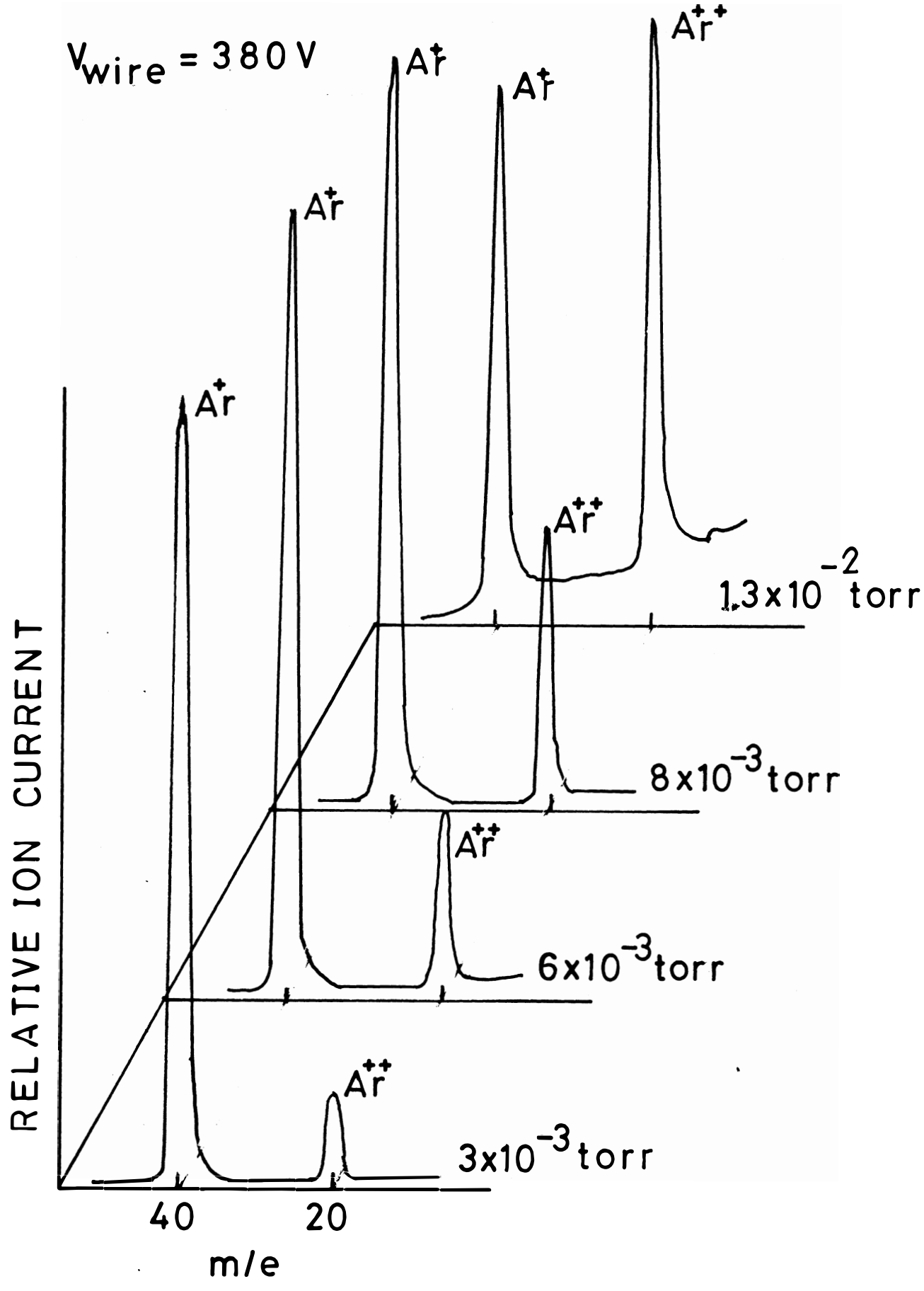
PURE ARGON
V_{wire} = 380 V
Ar^+
Ar^+
Ar^+
Ar^+
Ar^{++}
Ar^+
Ar^{++}
Ar^{++}
Ar^{++}
1.3×10^{-2} torr
8×10^{-3} torr
6×10^{-3} torr
3×10^{-3} torr
RELATIVE ION CURRENT
40
20
m/e

FIGURE 10

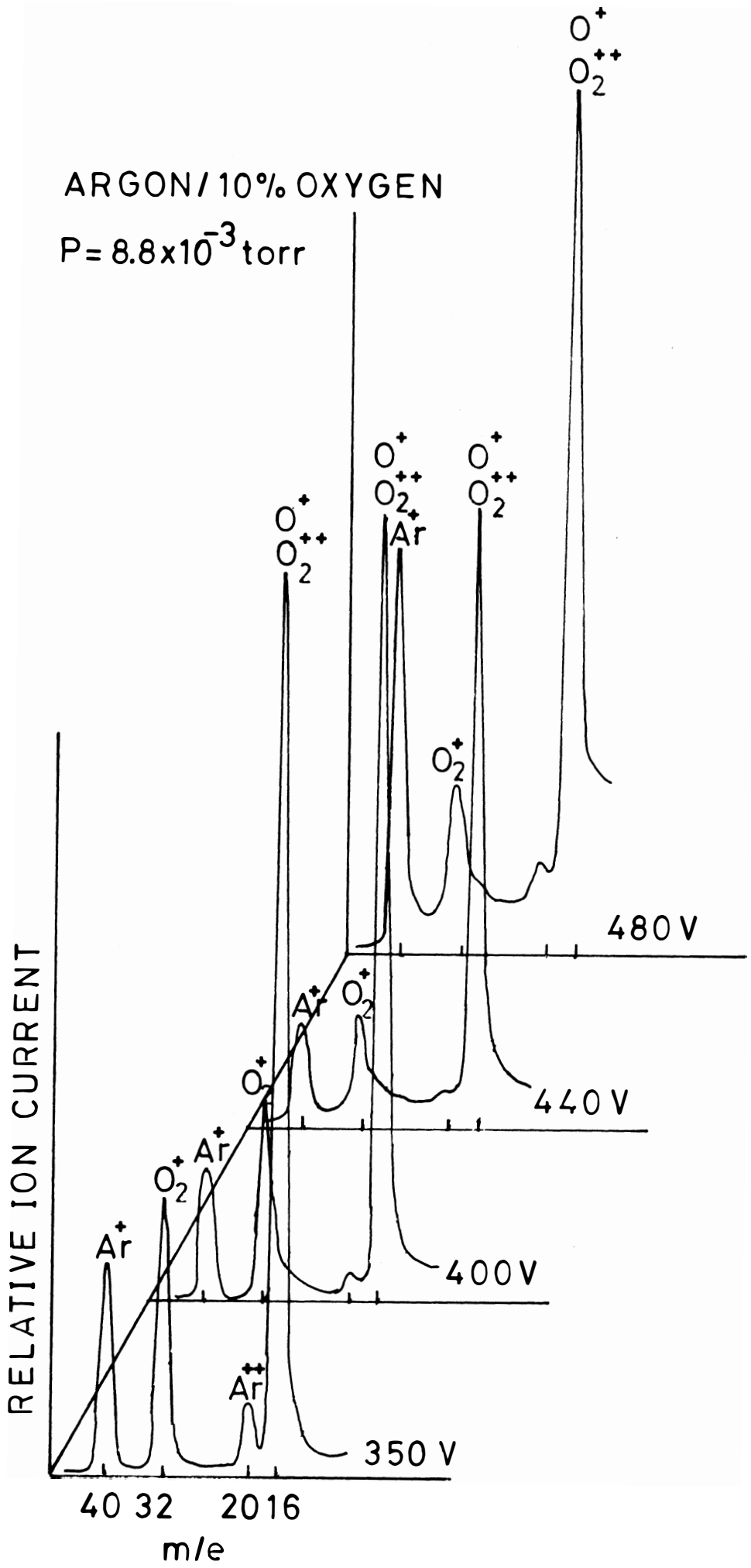
ARGON / 10% OXYGEN
P = 8.8x10^-3 torr
O+
O2++
Ar+
O2+
480 V
440 V
400 V
350 V
RELATIVE ION CURRENT
40 32 20 16
m/e

FIGURE 11

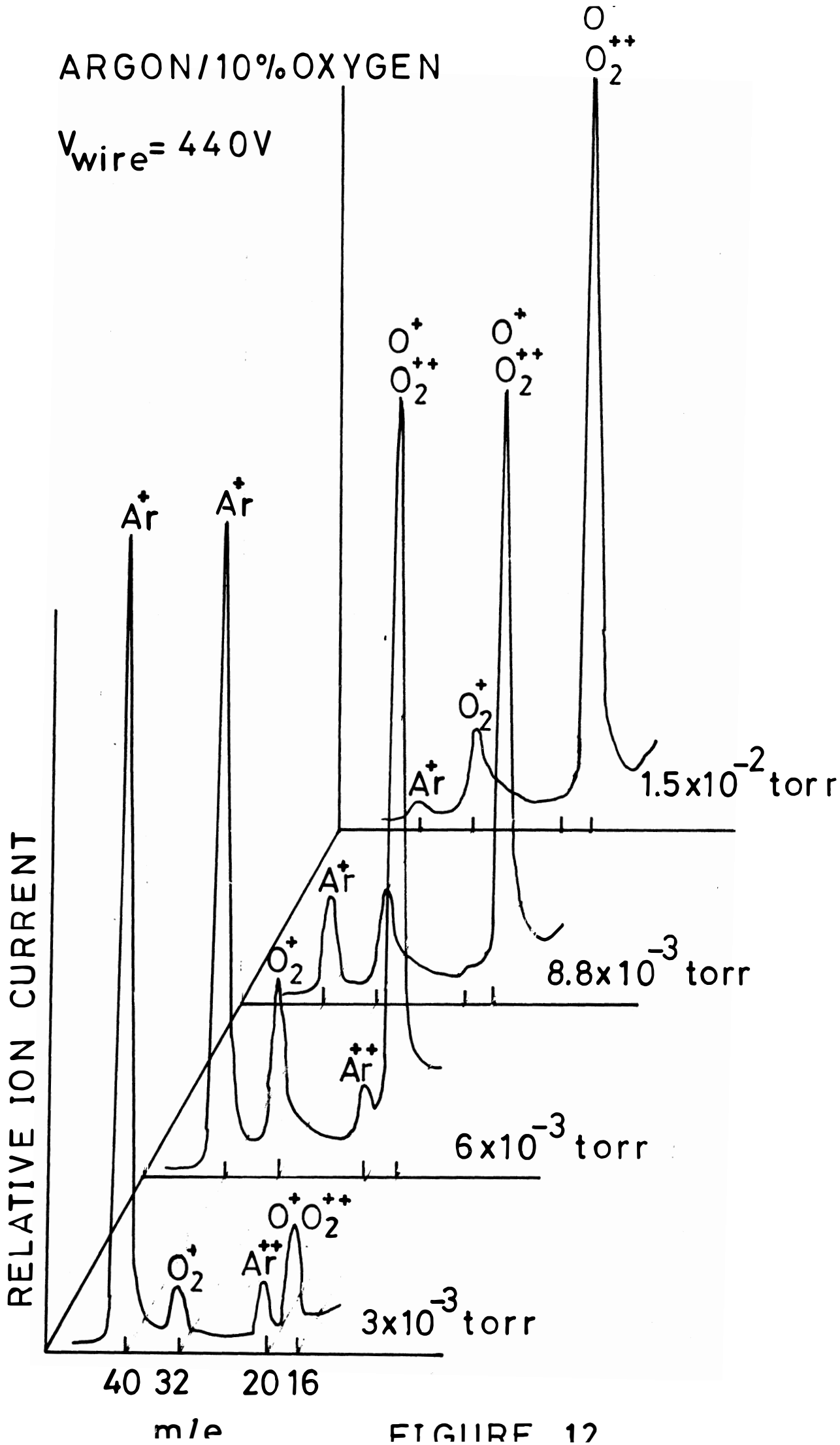
ARGON/10% OXYGEN
V_{wire}= 440V
O^+
O_2^{++}
Ar^+
O_2^+
Ar^{++}
1.5x10^{-2} torr
8.8x10^{-3} torr
6x10^{-3} torr
3x10^{-3} torr
RELATIVE ION CURRENT
40 32 20 16
m/e

FIGURE 12